

PSR J1311–3430: A HEAVYWEIGHT NEUTRON STAR WITH A FLYWEIGHT HELIUM COMPANION

ROGER W. ROMANI¹, ALEXEI V. FILIPPENKO², JEFFERY M. SILVERMAN², S. BRADLEY CENKO², JOCHEN GREINER³, ARNE RAU³,
JONATHAN ELLIOTT³, AND HOLGER J. PLETSCH⁴

To Appear in ApJL

ABSTRACT

We have obtained initial spectroscopic observations and additional photometry of the newly discovered $P_b = 94$ min γ -ray black-widow pulsar PSR J1311–3430. The Keck spectra show a He-dominated, nearly H-free photosphere and a large radial-velocity amplitude of 609.5 ± 7.5 km s⁻¹. Simultaneous seven-color GROND photometry further probes the heating of this companion, and shows the presence of a flaring infrared excess. We have modeled the quiescent light curve, constraining the orbital inclination and masses. Simple heated light-curve fits give $M_{NS} = 2.7 M_\odot$, but show systematic light-curve differences. Adding extra components allows a larger mass range to be fit, but all viable solutions have $M_{NS} > 2.1 M_\odot$. If confirmed, such a large M_{NS} substantially constrains the equation of state of matter at supernuclear densities.

Subject headings: gamma rays: stars — pulsars: general

1. INTRODUCTION

The bright γ -ray source 2FGL J1311.7–3429 has been known, and unidentified, since the early EGRET mission (Fichtel et al. 1994). After Romani (2012, hereafter R12) discovered an optical counterpart with a $P_b = 5626.0$ s (93.8 min) orbital period and evidence for very strong pulsar heating, Pletsch et al. (2012) managed to discover 2.5 ms Doppler-modulated pulsations in the *Fermi* Large Area Telescope (LAT, Atwood et al. 2009) γ -ray photons. Thus with orbital constraints, γ -only millisecond pulsars can be detected by the LAT, although PSR J1311–3430 was later found to also be intermittently visible in the radio (Ray et al. 2012, in prep.). Additional optical and X-ray observations supporting the orbital variability found above are described by Kataoka et al. (2012).

The γ -ray pulsar ephemeris gives an orbit of $a_{NS} \sin i = 0.010581$ lt-s for a minimum companion mass of $\sim 8 \times 10^{-3} M_\odot$. This measurement alone does not significantly constrain the neutron star mass, which is of particular interest, since van Kerkwijk, Breton, & Kulkarni (2011, hereafter vKKBK) found evidence that the original, $P_b = 9.2$ hr “black widow” (BW) binary PSR B1957+20 may host a remarkably heavy neutron star with $M_{NS} = 2.4 \pm 0.12 M_\odot$. If BW pulsars as a class are massive, PSR J1311–3430, with its ultra-short orbital period (the smallest of any rotation-powered pulsar), provides interesting opportunities for a mass determination.

We have been able to obtain exploratory spectroscopy and additional photometry that constrain properties of the PSR J1311–3430 system. These data show that the companion is a bloated, Roche-lobe filling substellar object whose photosphere is He dominated, with no detected H. While the neutron star mass estimate is quite model dependent, the data already imply that it is quite large. We discuss here the observations, the implications, and the prospects for further refine-

ment of the system parameters.

2. KECK LRIS SPECTROSCOPY

Six consecutive 300 s exposures of J1311–3430 were obtained with the Low Resolution Imaging Spectrometer (LRIS; Oke et al. 1995) at the Keck-I 10 m telescope on 2012 May 17 (UT dates are used herein; MJD 56064). We used the 1'' long slit at the parallactic angle (Filippenko 1982) and the 5600 Å dichroic splitter. In the blue camera the 600/4000 grism provided coverage to < 3400 Å at ~ 4 Å resolution; the red camera employed the 400/8500 grating for ~ 7 Å resolution. The seeing was good ($\sim 0.8''$) and conditions were nearly photometric. Standard processing and optimal extraction were applied; fluxes were calibrated against the red and blue standards BD+26°2606 and BD+28°4211, respectively.

These observations covered the phase of maximum light ($0.7 < \phi_B < 1.1$), so the spectrum is very blue (Figure 1). Although the temperature inferred from the color is $\gtrsim 10,000$ K (see §3), no Balmer lines are visible, implying an unusual surface composition. This is in contrast to the BW companions of PSR B1957+20 (vKKBK; Aldcroft, Romani, & Cordes 1992) and 2FG J2339-0533 (Romani & Shaw 2011), where relatively normal companion spectra are seen, with spectral classes appropriate to their (cooler) surface temperatures. After shifting the individual spectra to the rest frame using the sinusoidal approximate Doppler curve we obtain a phase-averaged spectrum dominated by narrow neutral He lines. We infer that this is the H-stripped remnant of an evolved stellar core.

The lower panel of Figure 1 shows the blue region of the normalized spectrum compared with a He-dominated model from the atmosphere grid of Jeffery, Woolf, & Pollacco (2001), smoothed to the resolution of the Keck data. The correspondence is excellent, with the exception that the Balmer lines, well visible in the model despite the 10^{-4} H number abundance, are undetectable in PSR J1311–3430. This implies a maximum H abundance $n(\text{H}) < 10^{-5}$.

We have used the model grid to estimate the effective temperature and gravity of this phase-averaged spectrum. The fit minima give $T_{\text{eff}} = 12,000 \pm 1000$ K and $\log g = 4.6 \pm 0.2$. Measurements of the equivalent width (EW) of individual lines are consistent with these conclusions; for example, the

¹ Department of Physics, Stanford University, Stanford, CA 94305, USA; rwr@astro.stanford.edu

² Department of Astronomy, University of California, Berkeley, CA 94720-3411, USA

³ Max-Planck-Institut für Extraterrestrische Physik, D-85748 Garching, Germany

⁴ Max-Planck-Institut für Gravitationsphysik (Albert-Einstein-Institut), D-30167 Hannover, Germany; Institut für Gravitationsphysik, Leibniz Universität Hannover, D-30167 Hannover, Germany

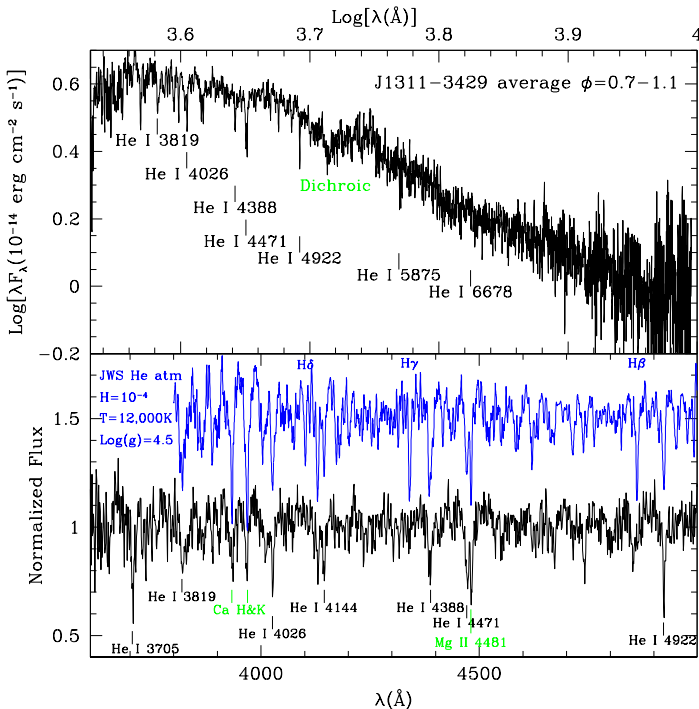


FIG. 1.— Combined, phased Keck LRIS spectrum. Upper Panel: Full spectrum. Lower panel: Spectrum showing He I line domination and the good match to the Jeffery, Woolf, & Pollacco (2001) model atmosphere (blue). ratio $EW_{4471}/EW_{4481} = 1.3 \pm 0.2$ and the absence of He II support the T_{eff} estimate, while the ratio $EW_{4471}/EW_{3819} = 1.97 \pm 0.2$ accords with the $\log g$ value. A few species, such as Si $\lambda 4552$ and Ni $\lambda 3995$, suggest some flux at lower values of $\log g$. This is not very surprising, since the companion is likely near-Roche-lobe filling with appreciable surface-gravity variation. Higher signal-to-noise ratio (S/N) spectra and synthetic composite spectral models will be needed to study the atmosphere’s surface variation.

The highly unusual He-dominated, low $\log g$ spectrum compromised attempts to find suitable cross-correlation templates. Accordingly, we adopt the best-fit atmosphere model to measure the radial velocities, using the RVSAO package in IRAF. All observed comparison stars were poor spectral matches and gave significantly lower correlation coefficients. However, all templates gave very similar radial velocities.

With the phase fixed by the pulsar-determined orbital ephemeris, we can fit a simple sinusoid to these velocities, obtaining amplitude $K_{\text{obs}} = 609.5 \pm 7.5 \text{ km s}^{-1}$ and average radial velocity $\Gamma = 62.5 \pm 4.5 \text{ km s}^{-1}$, with $\chi_{\nu} = 1.3$. At face value this gives a mass function

$$f_{2,\text{obs}} = \frac{K_{\text{obs}}^3 P_b}{2\pi G} = \frac{(M_{\text{NS}} \sin i)^3}{M_{\text{total}}^2} = 1.54 \pm 0.06 M_{\odot}$$

and a very large mass ratio $q_{\text{obs}} = (K_{\text{obs}}/K_{\text{NS}})^3 = 172.1 \pm 2.1$. However, the observed spectrum tracks the center of light (CoL) from the heated face of the companion, which has a smaller radial-velocity amplitude than the companion center of mass (CoM). For PSR B1957+20, vKBK estimate the correction factor as $K_{\text{cor}} = 1.09$ (i.e., $K_{\text{CoM}} = K_{\text{cor}} K_{\text{obs}}$). If we adopt this value of K_{cor} and the inclination constraint $i < 85^\circ$ from the lack of X-ray eclipses (R12; Kataoka et al. 2012), we derive $M_{\text{NS}} > 2.03 M_{\odot}$. This is an interestingly high mass for equation-of-state (EoS) constraints.

However, K_{cor} depends on the heating across the surface. Also, Romani & Shaw (2011) find that for the similar BW-

type binary J2339–0533, the heating introduces a significant non-sinusoidal component to the CoL curve, and it should be fit. Any further restrictions on the inclination i greatly narrow the pulsar mass range. These factors can be probed with light-curve modeling, so we have sought to improve the photometry to allow better constraints on the system masses.

3. GROND PHOTOMETRY

R12 measured the companion light curve from WIYN, SOAR, and archival VLT 3-band ($g'r'i'$ or BVI) photometry. However, the colors were not simultaneous; the largest dataset (SOAR Optical Imager $g'r'i'$) covered each filter on a separate night. These data showed significant epoch-to-epoch variability and large (up to 4 mag) flares, so precise measurements of the instantaneous colors were not available. Accordingly, we targeted J1311–3430 with the GROND system on the MPI/ESO 2.2 m telescope on La Silla (Greiner et al. 2008), obtaining simultaneous $g'r'i'z'$ JHK images starting 2012 July 09. The observations lasted 2.5 hr (~ 1.5 orbits) from MJD 56117.956 to 56118.059, covering two maxima (pulsar inferior conjunction). Twelve observation blocks were made, each with $4 \times 115 \text{ s}$ dithered optical pointings and $8 \times 60 \text{ s}$ near-IR exposures. The seeing was $\sim 1''$ and the air-mass increased slowly. Near maximum light, individual $g'r'i'z'$ exposures had adequate S/N, allowing a temporal resolution of $\sim 195 \text{ s}$, while at minimum and for all z' images 4 dithered exposures were combined to achieve adequate S/N. To ensure the best possible calibration of the optical bands, the target was revisited on 2012 August 10 with SDSS field exposures bracketing the J1311–3430 observations, allowing an accurate calibration of the field and target magnitudes; the calibration systematics are small compared to the photometric errors, and are included in the error flags of Figure 2 ($\sigma_{g'} \approx 0.02$, $\sigma_{r'} \approx 0.03$, $\sigma_{i'} \approx 0.05$ mag at maximum).

J1311–3430 had relatively low near-IR S/N and was detected at high significance only near maximum light; we thus made photometric measurements on an image stacked from frames covering phase ± 0.17 . The near-IR data were calibrated using 2MASS stars in the field, and transformed to AB magnitudes for spectral energy distribution (SED) fitting together with the optical data. These peak magnitudes were $J = 20.6 \pm 0.1$, $H = 21.1 \pm 0.3$, and $K = 20.9 \pm 0.3$. All magnitudes were corrected for the filter-specific dust-map-estimated Galactic extinction ($A_V = 0.173$ mag), using the Schlafly & Finkbeiner (2011) calibration.

Figure 2 summarizes the GROND photometry. The left panel shows the $g'r'i'z'$ light curves. The lower portion displays the $g' - i'$ color, blue at maximum and redder at minimum. The upper right shows the optical through near-IR SED at maximum light ($-0.1 < \phi_B < 0.1$) and the optical SED near quadrature ($\phi_B = 0.2\text{--}0.3, 0.7\text{--}0.8$). We see that at maximum the colors are comparable to those of a B7–B8 star in the blue, but there is a large near-IR excess. Although the pulsar heating makes the star multi-temperature, this very large excess suggests a large emitting area at low temperature. One source larger than the companion photosphere is the evaporative wind, where pulsar power may be reprocessed into the optical-IR. The optical light curves show appreciable fluctuations on short timescales. The lower-right panel summarizes this variability with the $g' - i'$ color plotted against the g' magnitude. Again the star is redder at fainter magnitudes. Interestingly, if we flag points that are brighter than the “quiescent” light-curve flux (see below), most of these points shift (green lines) to larger $g' - i'$ (redder) relative to the ex-

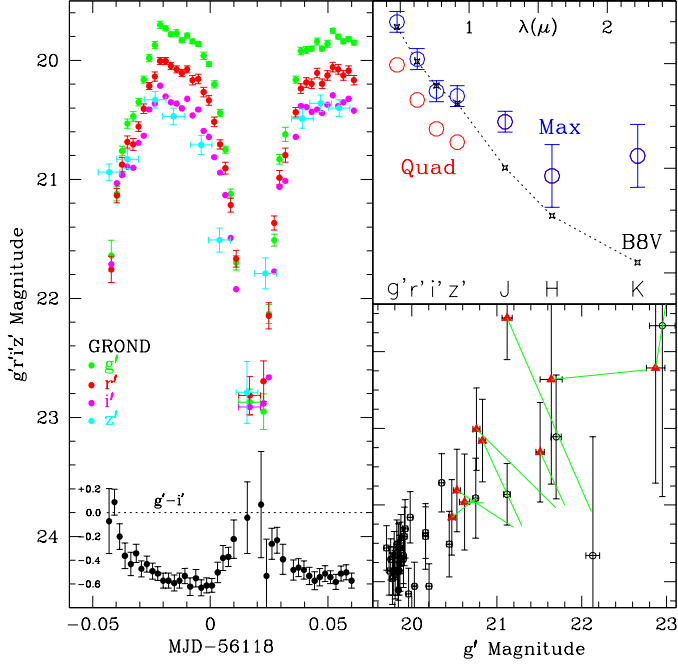


FIG. 2.— GROND photometry. Left: $g'r'i'z'$ light curves, showing reddening during minimum (pulsar superior conjunction). Upper right: The companion SED at maximum (phases -0.1 to 0.1 , blue points) and quadrature (phases 0.2 – 0.3 and 0.7 – 0.8 , red points). Comparison with a B8 star shows a large IR excess. Bottom right: J1311–3430 color variations. The redder spectrum at minimum is visible. Green lines and red triangles mark when an epoch has $\Delta g' > 0.2$ mag over the quiescent magnitude. Such flares show substantial increases in $g' - i'$.

pected quiescent color. An extreme example is the very large i' flare recorded by R12. We conclude that the principal light-curve fluctuations have a red SED. This implicates modulation in reprocessed pulsar emission by the variable wind off the companion. An alternative fluctuation site, stellar flares on the tidally locked companion, would in contrast be very hot (blue).

4. ELC MODELING AND PARAMETER ESTIMATION

The GROND data provide an instantaneous color reference for the longer, higher precision, but non-simultaneous SOAR light curves from MJD 56008.2–56010.4. Just as the GROND data exhibit red flares above the “quiescent” flux, comparing SOAR $g'r'$ photometry from adjacent orbits reveals several ~ 20 min flaring periods. In Figure 3 we plot the phased SOAR/GROND photometric points. During the first period all $g'r'$ measurements and errors are shown — “flaring” points (at $\phi_B = 0.15$ – 0.35 and 0.45 – 0.8) are plotted as crosses. During the second period we display only the quiescent points, but include the GROND $i'z'$ quiescent data. All SOAR i' were affected by strong flaring.

To constrain the system properties we have fit these “quiescent” light curves along with the radial-velocity measurements, using the “Eclipsing Light Curve” (ELC) code of Orosz & Hauschildt (2000). Typically, the code computes filter colors from atmospheres of the “NextGen” library (Hauschildt et al. 1999), but we found that these did not match the data well, plausibly due to the He domination of the photosphere. Instead, we fit using blackbody emissivities which gave reasonable light curves and colors. All fits used the γ -ray-determined phasing and pulsar projected semimajor axis.

There are five basic fit parameters: the system mass ratio $q = M_{\text{NS}}/M_c$, the pulsar irradiation modeled here as

an isotropic flux L_X , the companion’s underlying temperature T_1 and Roche-lobe fill factor f_1 , and the orbital inclination i . L_X is quite well constrained by the $g' - r'$ and $r' - i'$ colors near maximum light, giving $\log(L_X) = 35.3$. This is in accord with the spectroscopically estimated $T_{\text{eff}} = 12,000$ K near maximum. We also find that the secondary is very close to Roche-lobe filling in all acceptable fits, so we set $f_1 = 0.99$. We therefore adjusted the three remaining parameters to fit the light curves and spectral points. The very small photometric errors near maximum, coupled with stochastic variability, meant that even the best fits had formal $\chi^2/dof \approx 9$, so the T_1 and i error estimates come from the range giving a $\Delta\chi^2$ increase of $(\chi^2/dof)_{\text{min}}$ around the fit minimum. For q (and M_{NS}) the value (for a given fit i) is controlled by the radial-velocity measurements. These had $(\chi_v^2/dof)_{\text{min}} \approx 1.5$, so the error range was estimated from this smaller χ_v^2 increase.

For both PSR B1957+20 (Reynolds et al. 2007) and J2339–0533 (Romani & Shaw 2011) the photometric data are limited, and simple models with a pulsar-heated hemisphere gave adequate light-curve fits. In contrast, the flat light-curve maxima of J1311–3430 produce relatively poor fits to such models (R12). The best fit (Table 1) has a 60° inclination, resulting in a rather large pulsar mass, but the peak is too narrow, the minimum is too bright by ~ 1 mag, and the predicted K_{obs} is 2.2σ below the measured value.

Adding equatorial hot spots to the companion surface bracketing the L1 point (30° radius at 35° and -65°) can broaden the light-curve peak. This mimics equatorially concentrated heating, which may be plausibly invoked, as there is strong equatorial concentration in pulsar wind nebula (PWN) flows, giving rise to PWN tori. Alternatively, these asymmetric components may represent reprocessed pulsar flux in

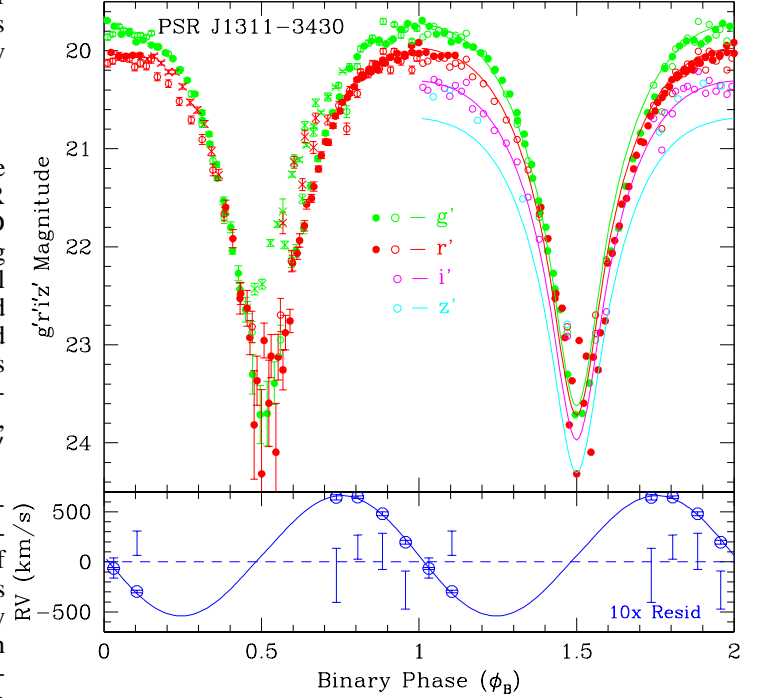


FIG. 3.— Top: SOAR (filled points) and GROND (open points) photometry; $g'r'$ “flare” measurements are flagged as crosses. Points during the second period exclude flare epochs. Curves are from the “L1 Spot” ELC fit. Bottom: Keck radial-velocity measurements, aligned with the light curve. Residuals are shown amplified by a factor of 10. The curve is from the same “L1 Spot” fit.

TABLE 1
ELC FIT PARAMETERS

Parameter	Basic LC	L1 Cold Spot	Eq Hot Spots
i [°]	60.4 ± 0.4	67.3 ± 0.3	57.9 ± 0.3
T_1 [K]	3440 ± 50	< 2000	< 1600
q	179.7 ± 3.9	177.1 ± 3.2	180.2 ± 3.3
$M_{\text{NS}} [M_\odot]$	2.68 ± 0.14	2.15 ± 0.11	2.92 ± 0.16
K_{cor}	1.06	1.04	1.06

a companion wind outflow. With these added components the model is a good match to the $g'r'i'$ light curves. The heated equator allows slightly lower $\log(L_X) = 35.0$, but the $K_{\text{cor}} = 1.06$ is large and the best-fit inclination is small, giving a very (possibly unphysically) large mass.

If, in contrast, we *cool* the region near L1, by applying a 40° spot with $1/2$ the local T , we also flatten the maxima. In this case, the CoL moves toward the CoM, resulting in a small $K_{\text{cor}} = 1.04$ and larger i . These two effects allow a neutron star mass of $2.15 M_\odot$. The fit quality is good, albeit with higher χ^2 than the equatorial spot model. This scenario gives the smallest M_{NS} of any viable fit. Such decreased L1 flux might plausibly arise from large limb and gravity darkening effects in the He-dominated atmosphere. We thus attempted to flatten the light curve by invoking extreme gravity darkening coefficients, as have been claimed for some semidetached binaries (Nakamura & Kitamura 1992). This allowed intermediate inclination and masses; for example, for $\tau_{\text{gr}} = 0.5$, we find $i = 63^\circ$ and $M_{\text{NS}} = 2.30 M_\odot$. For all cases the fit models underpredict the z' flux. This is likely related to the extra IR component seen in Figure 2.

5. DISCUSSION AND CONCLUSIONS

It is clear that additional physics is needed to fully model the light curve. Certainly, specific intensities from an appropriate He model grid would be useful. However, a good fit may also require some asymmetry in the heating, or re-processing of pulsar flux to produce optical/IR emission from the companion wind. We conclude that, at present, model assumption systematics dominate the statistical fit errors and preclude accurate mass determination. Nevertheless, the large mass function of PSR J1311–3430 virtually guarantees a large M_{NS} . In this it joins B1957+20, supporting the suggestion of vKBB that BW pulsars as a class may have high masses. The challenge is that secondary spectroscopy-derived estimates for these BW masses inevitably have substantial systematic uncertainty. In this sense, the mass estimates cannot match the “gold standard” timing-based $M_{\text{NS}} = 1.97 \pm 0.04 M_\odot$ for PSR J1614–2230 (Demorest et al. 2010). However, since EoS constraints tighten rapidly as the minimum required M_{NS} exceeds $2 M_\odot$, it is worth considering the prospects for refining the J1311–3430 mass estimate.

Figure 4 shows the present situation in the mass-mass plane. Compared to PSR B1957+20, J1311–3430 has a larger observed mass function ($1.54 M_\odot$ vs. $1.34 M_\odot$). However, our models give substantially smaller K_{cor} than assumed for PSR B1957+20, so in this sense our mass fits are conservative. The remaining systematic uncertainties in the light-curve shape allow inclinations $57^\circ < i < 67^\circ$. This large range dominates the systematic mass uncertainty. The best hope for eliminating otherwise plausible models and reducing the systematics lies with additional spectroscopy. Full-orbit coverage will, at minimum, substantially decrease the uncertainty in q . We also expect to detect the non-sinusoidal radial-velocity com-

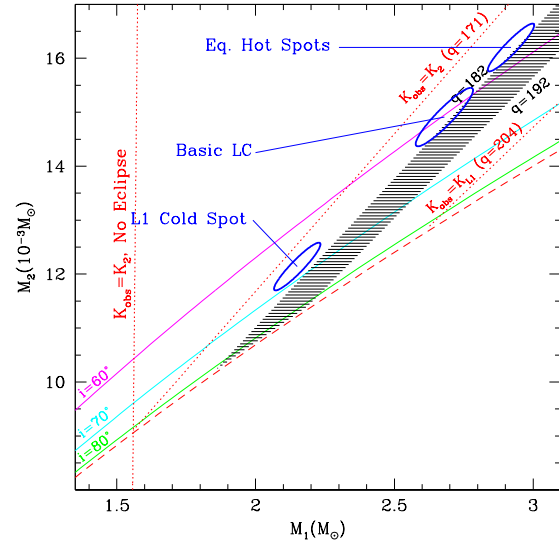


FIG. 4.— Mass constraints on the PSR J1311–3430 system. The pulsar mass function gives the solid diagonal lines for various inclinations i . The dotted vertical line gives the minimum from the companion mass function. The K_{cor} increase of the observed radial velocity is critical: we show the physically allowed range from the Keck data (dotted diagonal red lines, labeled by the appropriate value of q for J1311–3430), along with the range for PSR B1957+20 preferred by vKBB ($K_{\text{cor}} = 1.06$ – 1.13 ; shaded region). Fit regions for the three models in Table 1 are indicated with blue ellipses.

ponent, and with sufficient spectral resolution, the variations in absorption-line profile expected as the visible heated surface varies. Additional simultaneous multicolor photometry from many epochs could further isolate the photospheric light curve from a variable wind component. Deep multicolor images can constrain the residual illumination at pulsar superior conjunction, with additional i constraints. Of course, improved models are needed to fully exploit such data.

Our data also illuminate several other aspects of this unique system. The IR-dominated variability likely probes the extremely dense wind flux. Correlation with periods of radio-pulse visibility could be very revealing. The ultra-low-mass He companion points to unusual evolution, with substantial mass transfer and irradiative stripping of the core of an evolved secondary. Benvenuto, De Vito, & Horvath (2012) describe such a scenario, giving parameters remarkably similar to those of J1311–3430. This model’s slow mass transfer should allow substantial neutron star mass growth. Interestingly, for the large neutron star masses indicated here, the EoS must be very “stiff.” This means that for $M_{\text{NS}} \approx 2.5 M_\odot$, we can have a moment of inertia as large as $\sim 4 \times 10^{45} \text{ g cm}^2$ (Lattimer & Prakash 2007). This increases the spindown power of J1311–3430 from $\dot{E} = I\Omega\dot{\Omega} = 5 \times 10^{34} \text{ erg s}^{-1}$ (for $I_{45} = 1$), accommodating the large heating flux inferred from the peak colors and spectroscopic T_{eff} , even without equatorial concentration.

In summary, PSR J1311–3430 presents a number of unique properties that make it a potential Rosetta Stone for irradiation-driven evolution in tight binaries. If we can reduce the allowed model space, it seems likely to provide some of the most important constraints on the EoS of dense matter. And, even if PSR J1311–3430 or PSR B1957+20 do not provide the final word on the EoS, it is worth remembering that *Fermi* has proven to be an excellent finder of short- P_b BW systems, including detection via γ -ray-blind searches. Future studies of this extreme population may well provide a bullet-proof case for a stiff EoS.

We thank Jerry Oroc for helpful discussions on ELC model fitting, Simon Jeffery for alerting us to the He model atmospheres, and Vlad Sudilovsky for obtaining the GROND calibration observations. This work was partially supported by NASA grant NNX11AO44G. Part of the funding for GROND (both hardware and personnel) was generously allocated from the Leibniz-Prize to Prof. G. Hasinger (DFG grant HA 1850/28-1). A.V.F.'s group at U.C. Berkeley is supported

by Gary & Cynthia Bengier, the Richard & Rhoda Goldman Fund, the Christopher R. Redlich Fund, the TABASGO Foundation, and NSF grants AST-0908886 and AST-1211916. Some of the data presented herein were obtained at the W. M. Keck Observatory, which is operated as a scientific partnership among the California Institute of Technology, the University of California, and NASA; the Observatory was made possible by the generous financial support of the W. M. Keck Foundation.

REFERENCES

- Aldcroft, T. L., Romani, R. W., & Cordes, J. M. 1992, *ApJ*, 400, 638
Atwood, W. B., et al. 2009, *ApJ*, 697, 1071
Benvenuto, O. G., De Vito, M. A., & Horvath, L. E. 2012, *ApJ*, 753, L33
Covey, K. R., et al. 2007, *AJ*, 134, 2398
Demorest, P., et al. 2010, *Nature*, 467, 1081
Fichtel, K., et al. 1994, *ApJS*, 94, 551
Filippenko, A. V. 1982, *PASP*, 94, 715
Greiner, J., et al. 2008, *PASP*, 120, 405
Hauschildt, P. H., et al. 1999, *ApJ*, 525, 871
Jeffery, C. S., Woolf, V. M., & Pollacco, D. L. 2001, *A&A*, 376, 497
Kataoka, J., et al. 2012, *ApJ*, 757, 176
Lattimer, J. M., & Prakash, M. 2007, *PhR*, 442, 109L
Nakamura, Y., & Kitamura, M. 1992, *ApSS*, 191, 267
Nolan, P. L., et al. 2012, *ApJS*, 199, 31
Oke, J. B., et al. 1995, *PASP*, 107, 375
Orosz, J. A., & Hauschildt, P. H. 2000, *AA*, 364, 265
Pletsch, H., et al. 2012, *Science*, in press
Reynolds, M. T., et al. 2007, *MNRAS*, 379, 1117
Romani, R. W. 2012, *ApJ*, 754, L25 (R12)
Romani, R. W., & Shaw, M. S. 2011, *ApJ*, 743, L26
Schlafly, E. F., & Finkbeiner, D. P. 2011, *ApJ*, 737, 103
van Kerkwijk, M. H., Breton, R. P., & Kulkarni, S. R. 2011, *ApJ*, 728, 95 (vKKB)